

# INTERACTION OF COUPLED SPIN MOMENTS AND THE HIGH- $T_c$ SUPERCONDUCTING STATE

R. V. Helmolt, L. Haupt, Ch. Zock, and K. Bärner

4. Phys. Institut der Universität Göttingen, Bunsenstr.11-15, D-3400 Göttingen, FRG

**I. Introduction.** With the discovery of high  $T_c$  superconductors in oxide based metallic compounds the question of the interaction of spin moments with the high  $T_c$  superconducting state obtained renewed interest. One obvious question, in particular, would be a possible coexistence or exclusion of the superconducting and ferromagnetic collective states which might prove to be important for FM-SC layer structures to be used for thermal switching or ultrasonic wave amplification [1].

One may find the corresponding phase transition lines in a mixed crystal series, whose one end member is a high  $T_c$  superconductor and the other a metallic ferromagnet on an oxide basis; such ferromagnets have been known for quite a while [2,3] and at that time have been characterized as double exchange ferromagnets, because of the particular, double exchange (DE) coupling mechanism [4] involved; one example is  $\text{La}_{0.8}\text{Sr}_{0.2}\text{MnO}_3$ , where the  $\text{La}^{+3} : \text{Sr}^{+2}$  mixture is thought to introduce a  $\text{Mn}^{+3} : \text{Mn}^{+4}$  mixture, the basis for the DE coupling.

## II. Mixed crystal series. 1. $\text{La}_{0.8}\text{Sr}_{0.2}\text{Cu}_x\text{Mn}_{1-x}\text{O}_3$

When we, accordingly, set out to make the mixed crystal series  $\text{La}_{0.8}\text{Sr}_{0.2}\text{Cu}_x\text{Mn}_{1-x}\text{O}_3$ , we indeed found  $\text{La}_{0.8}\text{Sr}_{0.2}\text{MnO}_{3+\delta}$  to be a single phase metallic ferromagnet (fig. 1), but the compound with nominal composition  $\text{La}_{0.8}\text{Sr}_{0.2}\text{CuO}_{3+\delta}$ , although showing a Meissner effect and a resistivity drop [5], contained foreign phases suggesting a shift towards the "Zürich"-compound  $\text{La}_{1.8}\text{Sr}_{0.2}\text{CuO}_4$ , thus excluding this system to show a FM-SC transition line. As, however, single phase mixed crystals were obtained up to 40 at % Cu, the approach

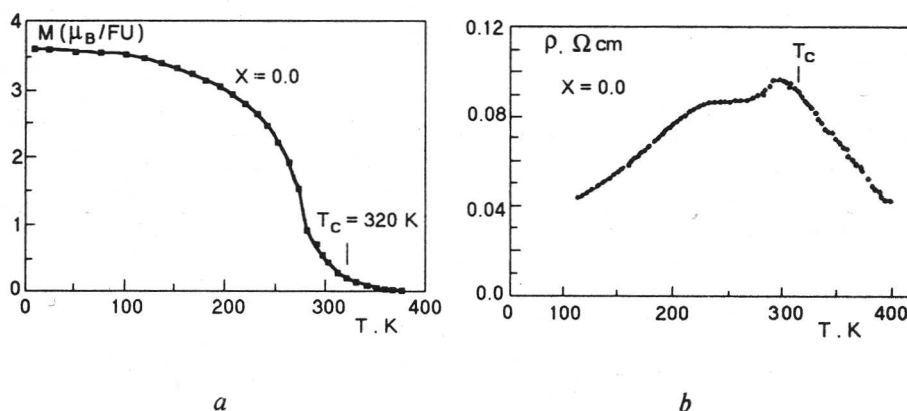


Fig. 1. Magnetic moment  $M(a)$  and resistivity  $\rho(b)$  of  $\text{La}_{0.8}\text{Sr}_{0.2}\text{MnO}_3$  versus temperature

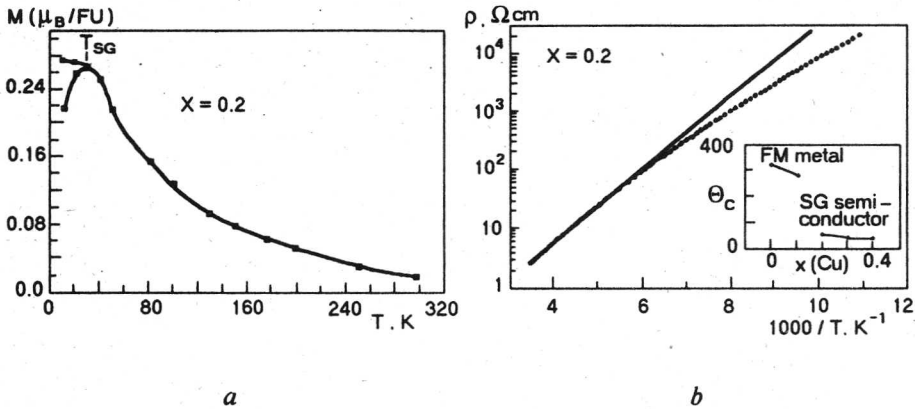


Fig. 2. Magnetic moment  $M(a)$  and resistivity  $\rho(b)$  of  $\text{La}_{0.8}\text{Sr}_{0.2}\text{Mn}_{0.8}\text{Cu}_{0.2}\text{O}_3$  versus temperature. Inset:  $T-x$  magnetic phase diagram of  $\text{La}_{0.8}\text{Sr}_{0.2}\text{Mn}_{1-x}\text{Cu}_x\text{O}_3$  mixed crystal.  $\theta_c$  pm Curie temperature

did not seem hopeless at this stage. However, we encountered another difficulty, which apparently is typical for mixed crystal series of this kind, i.e. a transition of the metallic ferromagnetic state into a semiconducting spin-glass-like state, here at a composition close to 15 at % Cu. For a characterization of that state, fig. 2 shows the conductivity of a sample with 20 at % Cu together with its zero field-(ZFC) and field cooled (FC) magnetization, while the inset of fig. 2 shows the magnetic phase diagram of this mixed crystal series.

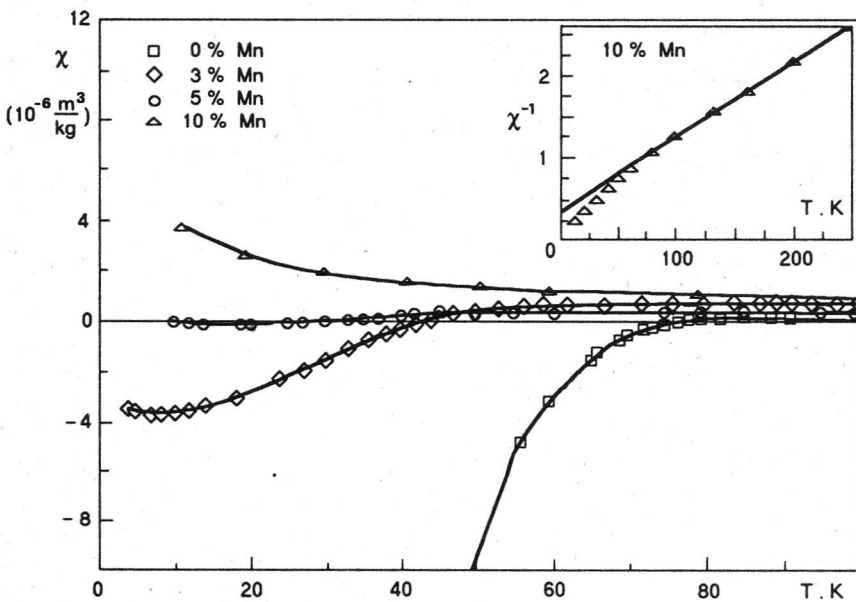


Fig. 3. Magnetic moment  $M$  of  $\text{La}_{(2-x)/3}\text{Ba}_{(1+x)/3}\text{Mn}_{1-x}\text{Cu}_x\text{O}_{3+\delta}$  mixed crystals versus temperature:  $x = 0, 3, 5, 10$  at % Mn. Inset: reciprocal susceptibility versus  $T$  for  $x = 10$  at % Mn

2.  $\text{La}_{(2-x)/3}\text{Ba}_{(1+x)/3}\text{Mn}_{1-x}\text{Cu}_x\text{O}_{3+\delta}$  . 2.1. Magnetization

A second attempt, i.e.  $\text{La}_{(2-x)/3}\text{Ba}_{(1+x)/3}\text{Mn}_{1-x}\text{Cu}_x\text{O}_{3+\delta}$  , proved to be more successful [6,7]. Here, the "chemical" degrees of freedom were considered; in particular, one can start with the "correct" La: Ba ratio at the SC side (fig. 3,4a,b)

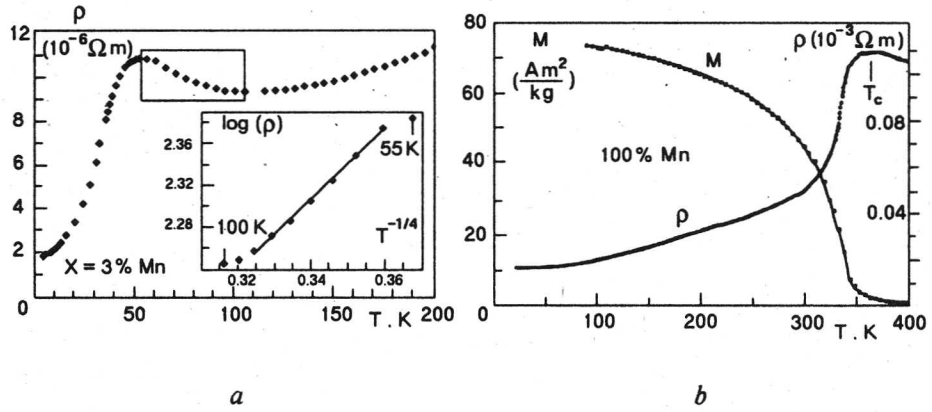


Fig. 4. Resistivity  $\rho$  of  $x = 3$  at % Mn (a) and (b)  $M(T)$  and  $\rho(T)$  of  $\text{La}_{0.67}\text{Ba}_{0.33}\text{MnO}_3$  . Inset (a):  $\log(\rho)$  versus  $T^{-1/4}$

and shift it with  $x$  such a way that on arrival at the FM side a metallic double exchange ferromagnet is readily obtained (fig. 4,b); certainly, if this is to be successful, the oxygen content  $\delta$  has to adjust. Fig. 5 shows the phase diagram

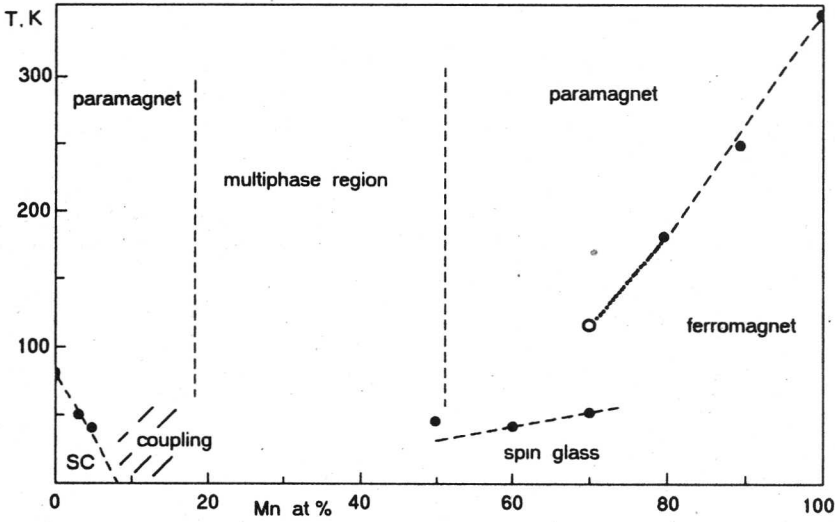


Fig. 5.  $T-x$  magnetic phase diagram of  $\text{La}_{(2-x)/3}\text{Ba}_{(1+x)/3}\text{Mn}_{1-x}\text{Cu}_x\text{O}_{3+\delta}$  mixed crystals

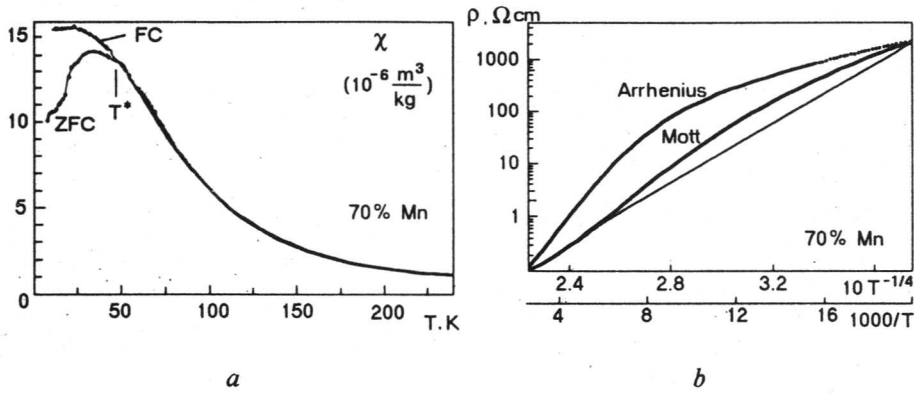


Fig. 6. Zero field (ZFC) and field cooled (FC) magnetic moment  $M$  (a) and resistivity  $\rho$ (ZFC) (b) (tentative Arrhenius and Mott plots) for  $x = 70$  at % Mn versus temperature

which is obtained: although a FM-SC phase separation line does not appear and there is a region where apparently mixed crystals do not exist, the phase diagram shows a symmetry which we would also obtain if we, naively, let a SC region border a FM region at  $x_c = 0.5$ . Note, that the FM-spin-glass (SG) transition on the FM side has its equivalent on the SC side, only the spin coupling — apparent as a slight curvature in  $\chi^{-1}(T)$  of the sample with 10 at % Mn (fig. 3) — is much weaker. The SG state near the FM side is again displayed by resistivity and magnetic moment

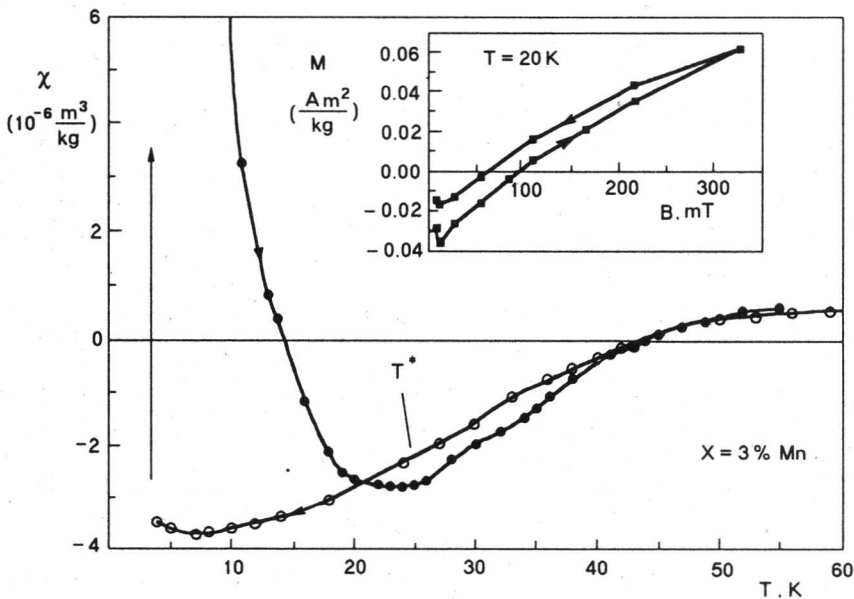


Fig. 7. Irreversible and reversible parts of the magnetic moment versus temperature for  $x = 3$  at % Mn: cooling at  $B = 11$  mT; arrow: application of 540 mT at 4.2 K; field reduction to 2 mT (after 2h); heating at 2 mT. Inset: magnetic moment versus field curve  $M(B)$  at 20 K

in fig. 6. The disappearance of FM appears to be connected with the disappearance of  $Mn^{+3}$  when  $Cu^{+2}$  is alloyed, predicting a change at 28.6 at % Cu [7].

If there is a magnetic coupling at 10 at % Mn, it could also exist at 5 at % or even at 3 at % Mn, where superconducting states are claimed below  $T_c$  (Fig's 3,4,5). Independent evidence for substitutional mixed crystals  $Cu_{1-x}Mn_x$  is obtained from diffraction data [6].

This opens up interesting speculations as to interactions between a spin-glass state and high- $T_c$  superconductivity. For that, however, one has to go back to the experimental evidence. Fig. 3 shows that the Meissner effect occurs in all three samples 0, 3, 5 at % Mn, its magnitude decreasing with  $x$ . Samples which contain Mn, however, show unusual relaxation effects in external magnetic fields: the magnetization of the sample with 3 at %, for example, when subjected to an external field  $H$  at  $T = 10$  K, shifts to a positive magnetization, which, after the field is removed, can only be inverted when the sample is heated (fig. 7). At  $T^*$ , in particular, the reversible branch of the  $M(T)$ -curve is reached.

This suggest a discrimination of field cooled (FC) and zero field cooled (ZFC)

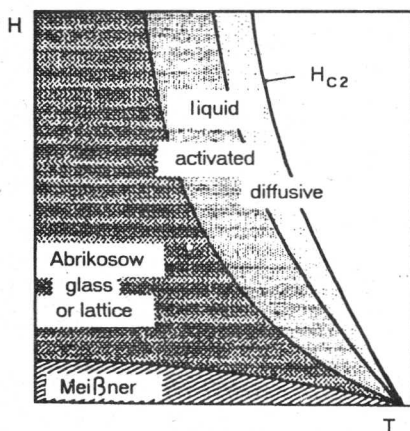


Fig. 8.  $H - T$  phase diagram of a Type II superconductor with thermal fluctuations according to [9,10,11]

$M(T)$ -curves and a "freezing" temperature ( $T^*$ ) also for this system. In contrast to a conventional spin-glass, however, the superconducting state appears to be involved.

High  $T_c$  superconductors have been recognized to be different from conventional superconductors in that the Shubnikov phase is considered to be split into an Abrikosov lattice (or glass) and an "Abrikosov liquid state" which is subdivided by diffusive and flux creep regimes when thermal fluctuations are considered [9,10,11] (fig. 8). Also, it is generally acknowledged, that granular superconductivity using weak links provide the random element necessary to invite the glassy state of high  $T_c$  superconductors [12]. This might be the case here, too,

but a second possibility appears now to be the interaction of random spins with the flux line distribution to give a double random system.

In order to make a judgement as to that one should compare the samples with and without Mn: when we consider the  $M(B)$  curve for  $x = 0$  (fig. 9,a),  $M$  is always negative, but a field hysteresis appears which has been assigned to flux trapping by other workers [13]. The  $x = 3$  at % sample, however, shows a completely different behaviour: when the magnetic field is stepped up and down symmetrically and the magnetization is allowed to relax for several minutes in between steps ( the sign of  $dM/dt$  is always that of  $dB/dt$ ), we obtain Fig. 9,b. Certainly one can obtain a cross-over to a positive magnetic moment when enough paramagnetic Mn atomic moments get aligned within the penetration depth of the magnetic field or—if we assume the superconductor to be in the mixed state—inside the normal conducting regions, but in that case one would equally expect a dealignment when the field is

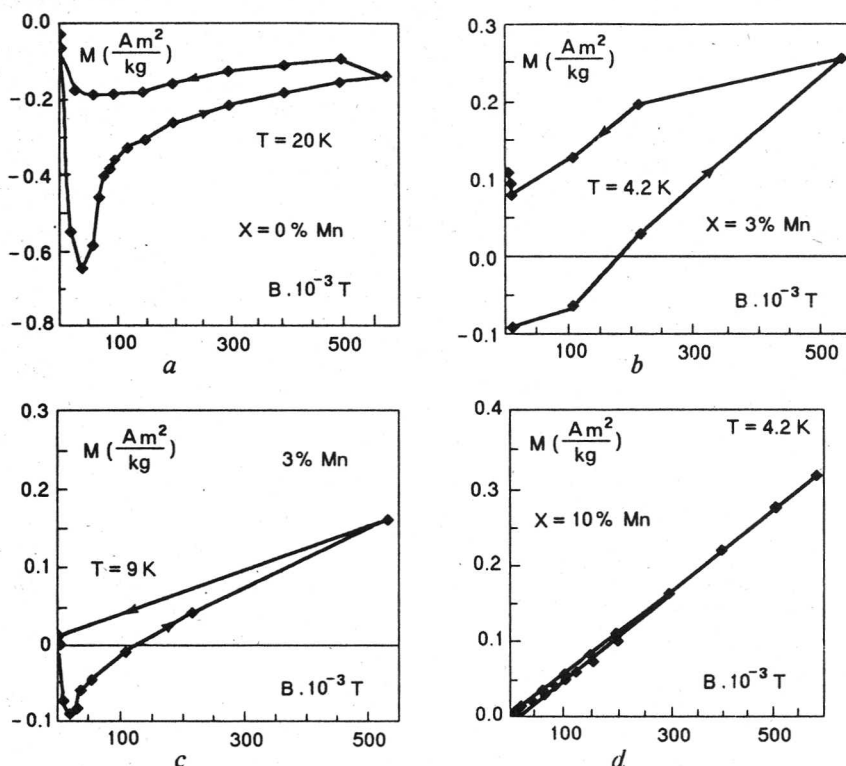


Fig. 9. Selected magnetization versus field curves  $M(B)$  for compounds with  $x = 0, 3, 10$  at % Mn

reduced, i.e. another zero crossing, eventually shifted by a slight hysteresis. This is indeed found for  $T > T^*$  (fig. 7, inset); for  $T < T^*$ , instead we observe a remanent magnetization, suggesting a coupling between the individual magnetic moments (fig's 9, b, c). Indeed, spin glasses often show a frozen in remanent magnetization by itself, which in our case might act as a (random) internal field, which cannot be excluded even when the external field  $B$  drops to zero (the small increase of  $M$  at low fields might be reminiscent of the Meissner phase).

## 2.2. Conductivity. 2.2.1. Variable range hopping

Below  $T_c$ , the resistivity of the superconducting sample with  $x = 3$  at %

(fig. 4, a) seems to follow an exponential law, suggesting flux creep [14], but because of the polycrystallinity of the sample we did not follow up with a more quantitative analysis. The slight drop of  $\rho$  for  $T > T_c$  can be assigned to variable

range hopping  $\rho \sim T^{-1/4}$  (see inset) in the normal (metallic) phase of the SC, as has been done with oxygen deficient samples of  $\text{YBa}_2\text{Cu}_3\text{O}_4$  [15]. Variable range hopping we also find for the spin-glass state at the FM side (fig's 2, 6), and even for the double exchange ferromagnet with  $x = 20$  at % Cu (fig. 10, a), again indicating a symmetry of the phases of the left and right side of the  $x - T$  diagram (fig. 5). For the end member DE-ferromagnets we do not find this behaviour; here  $\rho(T)$  looks like the inverse of the magnetization curve, suggesting magnon scattering (fig's 1, 4, b). There are, however, some details which seemingly do not fit into this

picture; i.e. the slight drop in  $\rho(T)$  for  $T > T_c$  (fig's 1,4,b) and the double maximum in  $\rho(T)$  for the DE ferromagnet  $\text{La}_{0.8}\text{Sr}_{0.2}\text{MnO}_3$ . The first finding can, however, be assigned to band splitting effects when the DE ferromagnetic long range order sets in [17], while the second effect might be due to the interaction of spin defects with a spin-polaron (see below), to give a decrease on carrier mobility.

### 2.2.2. Spin polarons

Both in the magnon scattering regime (fig.'s 1,10,b) and in the variable range hopping regime (fig. 10,a) of  $\rho$  shortly below  $T_c$  a relative maximum seems to be

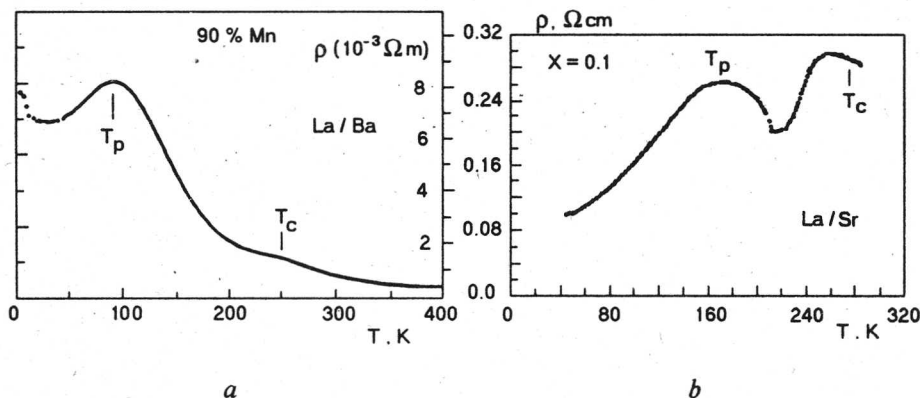


Fig. 10. Resistivity versus temperature for  $\text{La}_{0.37}\text{Ba}_{0.63}\text{Mn}_{0.9}\text{Cu}_{0.1}\text{O}_{3+\delta}$  (a) and  $\text{La}_{0.8}\text{Sr}_{0.2}\text{Mn}_{0.9}\text{Cu}_{0.1}\text{O}_3$  (b)  $T_c$ : Curie temperature,  $T_p$ : spin-polaron peak

superimposed. Both maxima are supposed to be due to spin-polarons. At first sight, this is astonishing since the conductivity type should not change inside the regime of long range order, i.e.  $0 < T < T_c$ .

However, if we consider that for the creation of a spin-polaron it is necessary to polarize the spin-lattice, this result can be readily understood. The magnetic polarisability can, for example, be characterised by the magnetic susceptibility (paraeffect) which in the case of ferromagnets indeed has a maximum shortly below  $T_c$ . Thus, as the range of the  $\rho(T)$  maxima appears to coincide with the easy

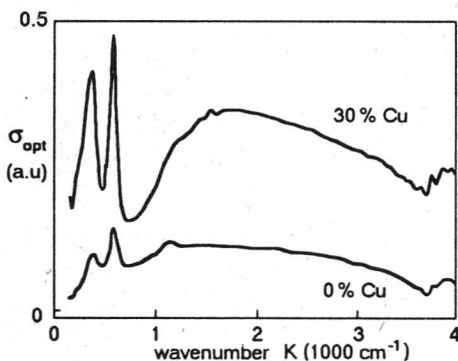


Fig. 11. Optical conductivity of  $\text{La}_{0.8}\text{Sr}_{0.2}\text{Mn}_{1-x}\text{Cu}_x\text{O}_3$  compounds at 300 K with  $x = 0, 30$  at % Cu versus wavenumber K

polarisability of the spin lattice, if the spin lattice is "molten",  $T > T_c$ , spin polarons are reduced to normal (evtl. spin-polarized) electrons and this also occurs for  $T \rightarrow 0$ , where the paraeffect disappears.

Non-adiabatic polaron hopping has been assigned to a broad maximum in the IR optical conductivity  $\sigma_{\text{opt}}$  of  $\text{La}_{2-x}\text{Sr}_x\text{CuO}_4$  compounds [16] and it is possible that spin-polaron hopping also shows in the IR-spectra.

Fig. 11 shows as a first result  $\sigma_{\text{opt}}$  of the semiconducting spin glass  $\text{La}_{0.8}\text{Sr}_{0.2}\text{Cu}_{0.3}\text{Mn}_{0.7}\text{O}_{3+\delta}$  as derived from the IR-reflectivity using a Kramers-Kronig analysis [8]. The spectrum is taken at 300 K, i.e. well above the freezing temperature where the spin-polaron is supposed to disappear and indeed spin polarons cannot be detected in the  $dc$ -conductivity. Therefore, the broad band at frequencies beyond the two "reststrahlen" peaks, if related to hopping, can only be normal polaron hopping. In the case of superconductors, even for the normal state, reststrahlen and polaron bands are much more difficult to detect in  $\sigma_{\text{opt}}$  as screening by the free carriers produces a structureless Drude-like behaviour. However, IR experiments are under way involving internal ( $T < T_c$ ) and external ( $H > 0$ ) polarisation in order to further investigate the spin-polaron hopping.

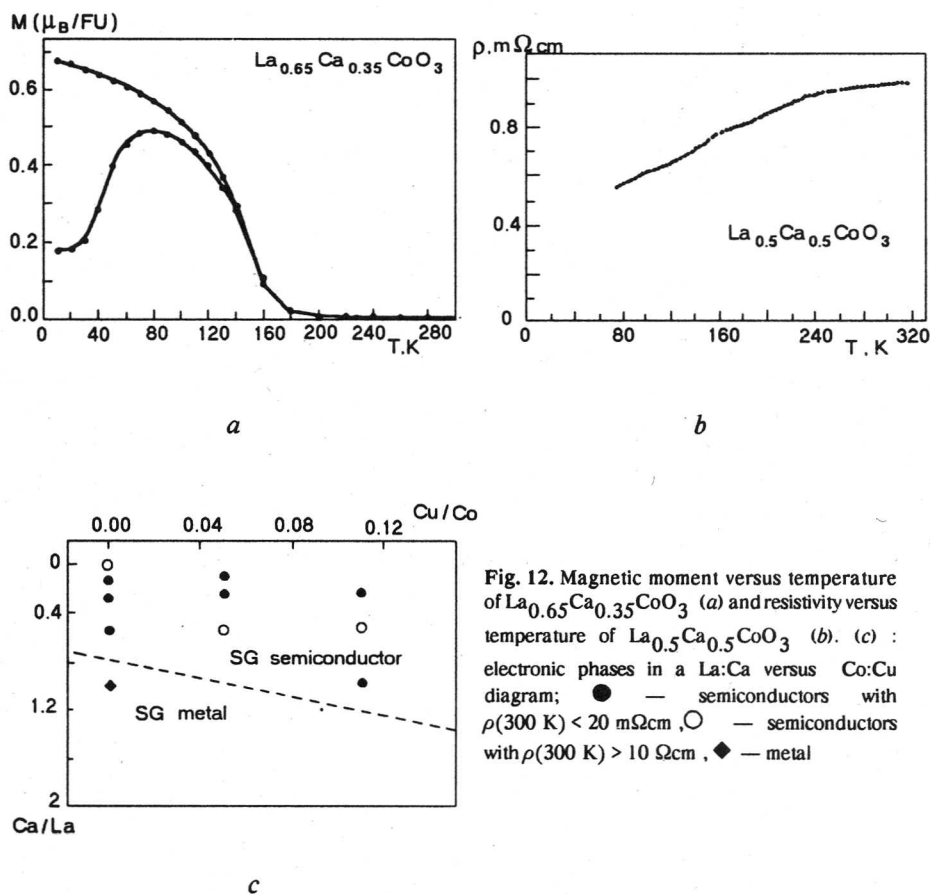


Fig. 12. Magnetic moment versus temperature of  $\text{La}_{0.65}\text{Ca}_{0.35}\text{CoO}_3$  (a) and resistivity versus temperature of  $\text{La}_{0.5}\text{Ca}_{0.5}\text{CoO}_3$  (b). (c) : electronic phases in a  $\text{La}:\text{Ca}$  versus  $\text{Co}:\text{Cu}$  diagram; ● — semiconductors with  $\rho(300\text{ K}) < 20\text{ m}\Omega\text{cm}$ , ○ — semiconductors with  $\rho(300\text{ K}) > 10\text{ }\Omega\text{cm}$ , ◆ — metal



### 3. Temperature-induced FM-SC transition

While a search for the FM-SC phase boundary appears to be problematic using mixed crystal series because of the random spin states which occur, one can still hope to find a temperature induced FM-SC transition in some compound.

Indeed, for samples of nominal composition  $\text{La}_1\text{Ca}_2\text{Co}_3\text{O}_{6+\delta}$  a large negative susceptibility has been reported at 227 K [18], more precisely in an applied field of 0.1 kOe and in a temperature region  $220 \text{ K} < T < 240 \text{ K}$ , which was bordered by a positive (ferromagnetic) susceptibility on both sides ("reentrant" ferromagnetism), but foreign phases were reported to be present.

In search of other temperature-induced FM-SC transitions, we have started to prepare some  $\text{La}_{1-x}\text{Ca}_x\text{Co}_{1-y}\text{Cu}_y\text{O}_{3-\delta}$  compounds, carefully checking for single phase crystallinity [19]. Fig. 12,c gives an overview by plotting the La:Ca ratio versus the Cu:Co ratio. All samples showed a spin-glass behaviour (fig. 12,a) probably due to the many random elements of these systems, i.e. the La/Ca and Cu/Co chemical mixtures, the induced valence mixture  $\text{Co}^{+3}/\text{Co}^{+4}$  and the high spin-low spin mixtures [20]. Also, most of the samples were insulators with variable range hopping conduction. We did, however, find one metallic compound (highest La/Ca ratio, fig. 12,b), indicating a metal-semiconductor boundary (dashed line in fig. 12,c), and suggesting that at higher La/Ca ratios one could ultimately find single phase compounds showing superconductivity and SC-FM boundaries.

#### Acknowledgements

The authors like to thank the Deutsche Forschungsgemeinschaft for partial support, Y. Tang and R. Braunstein for valuable discussions.

1. Anfinogenov V. B. et al., Sov. Phys. LJTP 15, 24 (1989).
2. Jonkerr G. H., Physica 22, 707 (1956).
3. Zener C., Phys. Rev. 82, 403 (1951).
4. Anderson P. W. and Hasegawa H., Phys. Rev. 100, 675 (1955).
5. Haupt L., Schunemann J.-W., Borner K., Sondermann U., Rager B., Addelouhab R.M., Braunstein R., Dong S., SSC 72, 1093 (1989).
6. Helmolt R. V., Haupt L., Borner K., SSC 80, 865 (1991).
7. Helmolt R. V., Haupt L., Borner K., Sondermann U., SSC 82, 693 (1992).
8. Haupt L., Helmolt R. V., Sondermann U., Borner K., Tang Y., Giessinger E.R., Ladizinski E., Braunstein R., Phys. Lett. A165, 473 (1992).
9. Huse D. A., and Seung H. S., Phys. Rev. B42, 1054 (1990).
10. Xing L., Tesanovic Z., Phys. Rev. Lett. 65, 794 (1990).
11. Fisher D. S., Fisher M. P. and Huse D. A., Phys. Rev. B43, 130 (1991).
12. Ebner C. and Stroud D., Phys. Rev. B31, 165 (1984).
13. Shcherbakov A. S. et al., Mod. Phys. Letters B4, 129 (1990).
14. Grishin A. M., Nicolaenko Yu. M., Zinovuk A. V., Vengalis B. U., Flodstrom A., Int. Symp. high  $T_c$  Superconductivity and Tunneling phenomena, Donetsk. (1992) p. 21
15. Medvedeva I. V. et al., Z. Phys. B81, 311 (1990).
16. Mihailovic D., Foster C. M., Voss K. and Heeger A. J., Phys. Rev. B42, 7989 (1990).
17. Mizzaferro J., J. Phys. Chem. Solids 46, 1339 (1985).
18. Tolpygo S. K. and Morozovskii A. E., Pis'ma Zh. Eksp. Teor. Fiz. 52, 1096 (1990).
19. Zock Ch., Diplomarbeit, Göttingen (1992).
20. Goodenough J. B., J. Appl. Phys. 37, 1415 (1966).